

Emergence of cosmological scaling behavior in asymptotic regime

M. A. Skugoreva,^{1,*} M. Sami,^{2,3,4,†} and N. Jaman^{2,‡}

¹Kazan Federal University, Kremlevskaya 18, Kazan, 420008, Russia

²Centre for Theoretical Physics, Jamia Millia Islamia, New Delhi-110025, India

³Maulana Azad National Urdu University, Gachibowli, Hyderabad-500032, India

⁴Institute for Advanced Physics & Mathematics, Zhejiang University of Technology, Hangzhou, 310032, China

In this paper we consider a scalar field system with a class of potentials given by the expression, $V(\phi) \propto \phi^m \text{Exp}(-\lambda\phi^n/M_{Pl}^n)$; $m \geq 0, n > 1$ for which $\Gamma = V_{\phi\phi}V/V_\phi^2 \rightarrow 1$ as $|\phi| \rightarrow \infty$. We carry out dynamical analysis for the underlying system choosing a suitable set of autonomous variables and find all the fixed points. In particular, we show that the scaling solution is an attractor of the system in the asymptotic regime. We indicate the application of the solution to models of quintessential inflation.

PACS numbers:

I. INTRODUCTION

Scalar fields have been used extensively in cosmology for the description of inflationary era as well as the phenomenon of late time acceleration. In their application to late time acceleration, it is imperative that they do not interfere with the thermal history of universe and the dynamics is such that the late time physics bears no dependence on initial conditions. The first requirement *à la* the nucleosynthesis constraint [1–4] implies that the field energy density should remain sub-dominant to background during radiation and matter era and should show up only at late stages to account for the late time acceleration. In general, the first requirement asks for a steep field potential where as the second forces the choice of a particular type of steep behavior. In case of the early field dominance, the field energy, during evolution, undershoots the background such that the Hubble damping freezes the scalar field ϕ on its potential.¹ As the background energy density becomes comparable to field energy density, field evolution commences again, hereafter, the evolution crucially depends on the nature of steepness of the field potential. In case the underlying field potential is of standard exponential type, the field energy density exactly tracks the background forever. If the potential is less steeper than the exponential, for instance the inverse power law potentials, the field energy density gradually approaches the background and overtakes it. And for potentials more steeper than the standard exponential, the field energy density would evolve away from the background pushing the field into freezing regime and after the recovery from the latter [5, 6], the same behavior keeps repeating till late.² Such a framework belongs to the class of thawing models [7, 8] where the evolution is sensitive to the initial conditions.

Recently, generalized exponential potential $V(\phi) \propto \text{Exp}(\lambda\phi^n/M_{Pl}^n)$, $n > 1$ was considered in Refs. [6, 9] in context of quintessential inflation [2, 5, 10–27] which successfully describes inflation and mimics desirable behavior [28–33] at late stages despite the fact that the slope of the potential is not constant which is important for the derivation of scaling solution. In this case one has an additional equation for the slope where crucial role is played by a quantity, $\Gamma = V_{\phi\phi}V/V_\phi^2$ [28] such that the latter being equal to one implies the standard case of exponential potential. There might be interesting cases in which Γ approaches unity in certain limits signaling the emergence of scaling behavior asymptotically; the mentioned class of potential satisfies the said criteria.

It is desirable to have scaling behavior in models of dark energy which makes the evolution free of initial conditions [28]. However, since the scaling solutions are not accelerating one needs late time exit from scaling regime to acceleration which can be triggered using various mechanisms discussed in the literature [22, 34]. Scaling behavior with mechanism of late time exit to acceleration dubbed *tracker* [28, 35–38] is at the heart of model building for dark energy and quintessential inflation.

*Electronic address: masha-sk@mail.ru

†Electronic address: samijamia@gmail.com

‡Electronic address: nurjaman@ctp-jamia.res.in

¹ In case, the field energy density is sub-dominant to the background initially, the field remains frozen till its energy density become comparable to the background, thereafter evolution depends upon the nature of steepness of the potential similar to the case described in the text.

² We imagine a late time feature in the potential allowing the exit to acceleration.

In this paper we consider a scalar field system with a generalized class of potentials with the desired property of Γ and carry out dynamical analysis to rigorously confirm the existence and stability of scaling solutions using the autonomous system framework; the analysis was missing in the earlier cited work. We also indicate the applications of these solutions for models of quintessential inflation.

II. DYNAMICAL ANALYSIS

In what follows we shall present the evolution equations in the autonomous form suitable for the study of fixed points. In particular, our focus will be on the existence and stability of the scaling solution which plays important role in model building of dark energy and quintessential inflation. Besides the autonomous form, we shall also retain evolution equations in the original variables which would be helpful in constructing certain physical quantities along with the additional check on the results to be obtained from the autonomous system. We shall use units $\hbar = c = 1$.

A. Equations of motion

Let us consider the model of quintessence with the following action

$$S = \int \sqrt{-g} d^4x \left[-\frac{M_{Pl}^2}{2} R + \frac{1}{2} (\nabla\phi)^2 - V(\phi) \right] + S_M, \quad (1)$$

where

$$V(\phi) = V_0 \phi^m e^{\frac{-\lambda\phi^n}{M_{Pl}^n}}; \quad \lambda > 0, V_0 > 0, n > 1, m \geq 0 \quad (2)$$

is the scalar field potential; $M_{Pl}^2 = \frac{1}{8\pi G}$ and S_M is the matter action. The case with $m = 0$ and $n = 1$ has been thoroughly studied in many literature [3, 15, 22, 39–41]. Several asymptotic solutions were found in [42] in the models with various parameters n, m of the potential (2). The mixed-quintessence potential similar to (2) appears in the Einstein-frame formulation of the nonminimal coupled scalar field models and it is obtained in the paper [43] that corresponding system shows a scaling behavior in spite of having a potential with not constant slope.

Hereafter, we specialize to a spatially flat Friedmann-Lemaître-Robertson-Walker metric $ds^2 = dt^2 - a^2(t)\delta_{ij}dx^i dx^j$, where a is the scale factor. Equations of motion are obtained by varying the action (1) with respect to metric and with respect to the scalar field giving rise to the usual set of evolution equations,

$$3H^2 M_{Pl}^2 = \frac{1}{2} \dot{\phi}^2 + V(\phi) + \rho, \quad (3)$$

$$(2\dot{H} + 3H^2) M_{Pl}^2 = -\frac{1}{2} \dot{\phi}^2 + V(\phi) - p, \quad (4)$$

$$\ddot{\phi} + 3H\dot{\phi} + V_\phi = 0, \quad (5)$$

where $H(t) \equiv \frac{\dot{a}}{a}$ is Hubble parameter, ρ, p — the energy density and pressure of the background matter, $w = p/\rho$ — the background matter equation of state parameter ($w \in [-1; 1]$) and $V_\phi = \frac{dV}{d\phi}$.

Let us note that the asymptotic scaling solution in the model with the potential $V(\phi) = V_0 e^{\frac{-\lambda\phi^n}{M_{Pl}^n}}$ was constructed in Ref. [9], though the existence and stability was not demonstrated there using dynamical system analysis. We could expect that this solution exists for a general potential $V(\phi) = V_0 \phi^m \text{Exp}\left(-\frac{\lambda\phi^n}{M_{Pl}^n}\right)$ also as the parameter $\Gamma \equiv V_{\phi\phi} V / V_\phi^2$ has the same asymptotic behavior in this case. This is not surprising as power law gives insignificant contribution in the asymptotic regime. In this case, we are interested to investigate all the fixed points, in particular, the scaling solution.

Let us note that the behavior of scalar field in the scaling regime is characterized by,

$$w_\phi = \frac{p_\phi}{\rho_\phi} = \frac{\dot{\phi}^2/2 - V}{\dot{\phi}^2/2 + V} = w \quad \Rightarrow \quad \dot{\phi}^2(1 - w) = 2(1 + w)V, \quad (6)$$

where ρ_ϕ , p_ϕ , w_ϕ are the energy density, the pressure and the equation of state parameter of the scalar field ϕ correspondingly. The time derivative from last relation in (6) is

$$\begin{aligned} \ddot{\phi}\dot{\phi}(1-w) = (1+w)V_\phi\dot{\phi} &\Rightarrow (-3H\dot{\phi} - V_\phi)\dot{\phi}(1-w) = (1+w)V_\phi\dot{\phi} \Rightarrow \\ &\Rightarrow -3(1-w)H\dot{\phi}^2 = 2V_\phi\dot{\phi}. \end{aligned} \quad (7)$$

Therefore, we find for the scaling solution

$$\frac{\dot{\phi}^2}{2V} = \frac{1+w}{1-w}, \quad \frac{V_\phi}{\dot{\phi}H} = \frac{3}{2}(w-1). \quad (8)$$

Some of the features of dynamics can be made clear by looking at the form of the potential. We plot the potential $V(\phi) = V_0\phi^m e^{\frac{-\lambda\phi^n}{M_{Pl}^2}}$ for several sets of the parameters n , m , λ , V_0 and $M_{Pl}^2 = 1$ and observe that for n even and m odd, the potential has minimum for negative value of the field and should give rise to de Sitter (see Fig. 2, right plot). However, this case can not be captured by our choice of autonomous variables; they are best suited to scaling solutions. In case of even $m > 0$ and both n being even or odd, the potential has local minimum at $\phi = 0$ with $V = 0$. In this case, we expect the stable fixed point would correspond to $\Omega_\phi \rightarrow 0$ corresponding to $w_{eff} = \frac{p+p_\phi}{\rho+p_\phi} \rightarrow w$. Thus apart from the scaling solutions, it is expected that the formalism would capture the latter behaviour also.

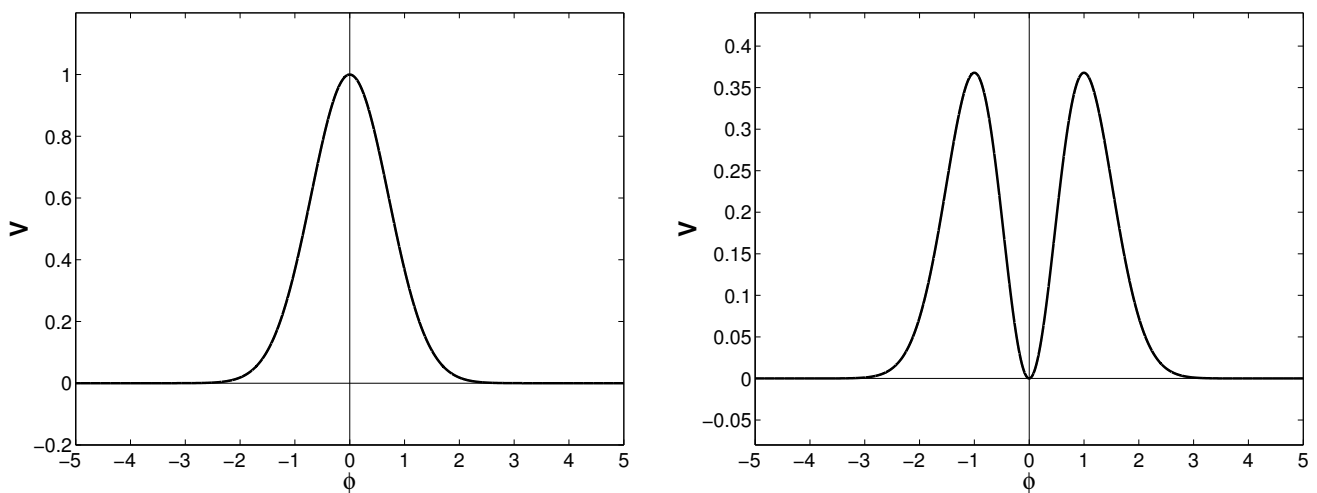


FIG. 1. The scalar field potential $V(\phi) = V_0 e^{\frac{-\lambda\phi^n}{M_{Pl}^2}}$ is plotted for the parameters $n = 2, m = 0$ (left) and $n = 2, m = 2$ (right). Other parameters are $V_0 = 1, \lambda = 1, M_{Pl}^2 = 1$.

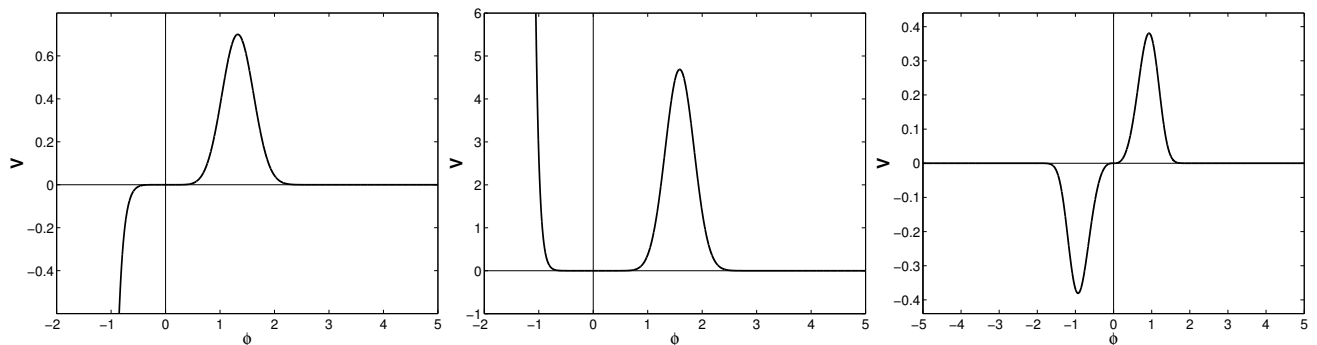


FIG. 2. The scalar field potential $V(\phi) = V_0 e^{\frac{-\lambda\phi^n}{M_{Pl}^2}}$ is plotted for the parameters $n = 3, m = 7$ (left), $n = 3, m = 12$ (middle) and $n = 4, m = 3$ (right). Other parameters are $V_0 = 1, \lambda = 1, M_{Pl}^2 = 1$.

We introduce new expansion-normalized variables x, y, A :

$$x = \frac{\dot{\phi}^2}{2V}, \quad y = \frac{V_\phi}{\dot{\phi}H}, \quad A = \frac{1}{\phi + 1}. \quad (9)$$

Let us note that the variable x is positive if $V(\phi) > 0$ and the variables x & y in Eq. (9) are constants in the scaling regime which exactly happens in the case of a standard exponential potential where the third relation is redundant. For a general class of potentials with a property, the parameter $\Gamma \rightarrow 1$ as $|\phi| \rightarrow \infty$, we have asymptotic scaling regime where A is zero.

The initial variables ϕ , H , ρ and also their time derivatives and expressions of these variables are expressed through autonomous variables x , y , A . Indeed, we have,

$$\phi = \frac{1-A}{A}, \quad (10)$$

$$\dot{\phi}^2 = 2xV(\phi) = 2xV_0 \left(\frac{1-A}{A} \right)^m e^{-\frac{\lambda(1-A)^n}{M_{Pl}^n A^n}}, \quad (11)$$

$$\begin{aligned} H^2 &= \frac{V_\phi^2}{y^2 \dot{\phi}^2} = \frac{V_0^2}{y^2 \dot{\phi}^2} e^{-\frac{2\lambda\phi^n}{M_{Pl}^n}} \left(m\phi^{m-1} - \frac{\lambda n}{M_{Pl}^n} \phi^{m+n-1} \right)^2 = \\ &= \frac{V_0}{2xy^2} e^{-\frac{\lambda(1-A)^n}{M_{Pl}^n A^n}} (1-A)^{m-2} A^{2-2n-m} \left[mA^n - \frac{\lambda n}{M_{Pl}^n} (1-A)^n \right]^2. \end{aligned} \quad (12)$$

Positive values of the scalar field ϕ correspond to $A \in (0; 1)$, negative those correspond to $A \in (-\infty; 0) \cup (1; +\infty)$ and $A \rightarrow \pm\infty$ for $\phi \rightarrow -1$.

Using definitions of x , y , A (9) and the expression (10) we derive the following important relations:

$$\frac{V}{2M_{Pl}^2 H^2} = \frac{xy^2}{M_{Pl}^2} A^{2n-2} \left[\frac{1-A}{mA^n - \frac{\lambda n}{M_{Pl}^n} (1-A)^n} \right]^2, \quad (13)$$

$$\begin{aligned} \frac{\dot{H}}{H^2} &= -\frac{3}{2}(w+1) + \frac{V}{2M_{Pl}^2 H^2} (x(w-1) + w+1) = \\ &= -\frac{3}{2}(w+1) + \frac{xy^2}{M_{Pl}^2} A^{2n-2} (x(w-1) + w+1) \left[\frac{1-A}{mA^n - \frac{\lambda n}{M_{Pl}^n} (1-A)^n} \right]^2, \end{aligned} \quad (14)$$

$$\frac{\ddot{\phi}}{\dot{\phi}H} = -y - 3, \quad (15)$$

$$w_\phi = \frac{x-1}{x+1}, \quad (16)$$

$$\begin{aligned} w_{eff} &= \frac{p+p_\phi}{\rho+p_\phi} = -\frac{(2\dot{H}+3H^2)M_{Pl}^2}{3M_{Pl}^2 H^2} = -1 - \frac{2}{3} \frac{\dot{H}}{H^2} = \\ &= w - \frac{2}{3} \frac{xy^2}{M_{Pl}^2} A^{2n-2} (x(w-1) + w+1) \left[\frac{1-A}{mA^n - \frac{\lambda n}{M_{Pl}^n} (1-A)^n} \right]^2, \end{aligned} \quad (17)$$

$$\rho_\phi = \frac{\dot{\phi}^2}{2} + V(\phi) = V_0(x+1) \left(\frac{1-A}{A} \right)^m e^{-\frac{\lambda(1-A)^n}{M_{Pl}^n A^n}}, \quad (18)$$

$$\begin{aligned} \rho &= 3H^2 M_{Pl}^2 - \rho_\phi = \\ &= \frac{3V_0 M_{Pl}^2}{2xy^2} e^{-\frac{\lambda(1-A)^n}{M_{Pl}^n A^n}} \left(\frac{1-A}{A} \right)^{m-2} \left[m - \frac{\lambda n}{M_{Pl}^n} \left(\frac{1-A}{A} \right)^n \right]^2 - V_0(x+1) \left(\frac{1-A}{A} \right)^m e^{-\frac{\lambda(1-A)^n}{M_{Pl}^n A^n}} = \\ &= V_0 \left(\frac{1-A}{A} \right)^{m-2} e^{-\frac{\lambda(1-A)^n}{M_{Pl}^n A^n}} \left\{ \frac{3M_{Pl}^2}{2xy^2} \left[m - \frac{\lambda n}{M_{Pl}^n} \left(\frac{1-A}{A} \right)^n \right]^2 - (x+1) \left(\frac{1-A}{A} \right)^2 \right\}, \end{aligned} \quad (19)$$

$$\Omega_\phi = \frac{\rho_\phi}{3M_{Pl}^2 H^2} = \frac{V}{3M_{Pl}^2 H^2} (x+1) = \frac{2}{3M_{Pl}^2} (x+1) xy^2 A^{2n-2} \left[\frac{1-A}{mA^n - \frac{\lambda n}{M_{Pl}^n} (1-A)^n} \right]^2. \quad (20)$$

Let us note that points of the phase space of new variable (x, y, A) have the physical sense only if their coordinates x_0, y_0, A_0 gives rise to $\rho \geq 0$ after the substitution to (19).

Let us emphasize that the parameter Γ becomes important beyond the standard exponential; it governs the dynamics of the underlying system. In general, it provides yardstick to check for the scaling solutions. For the potential under consideration, we have

$$\Gamma = 1 + (n-1) \frac{V}{V_\phi \phi} - mn \left(\frac{V}{V_\phi \phi} \right)^2 = 1 + \frac{(n-1)A^n}{mA^n - \frac{\lambda n}{M_{Pl}^n}(1-A)^n} - \frac{mnA^{2n}}{\left[mA^n - \frac{\lambda n}{M_{Pl}^n}(1-A)^n \right]^2}, \quad (21)$$

where we have used the following relation,

$$\frac{V}{V_\phi \phi} = \frac{A^n}{mA^n - \frac{\lambda n}{M_{Pl}^n}(1-A)^n}. \quad (22)$$

Let us note that $n = 1, m = 0$ corresponds to the standard case of an exponential potential which gives rise to scaling solution. It is interesting that $\Gamma \rightarrow 1$ for arbitrary values of n & m provided that $A \rightarrow 0$ corresponding to $|\phi/M_{Pl}| \rightarrow \infty$, which signals the emergence of scaling behavior in the asymptotic regime, while $\Gamma \rightarrow \frac{m-1}{m}$ in other asymptotic limit $\phi/M_{Pl} \rightarrow 0$ (that is $A \rightarrow 1$). In what follows, we shall demonstrate this rigorously.

Taking the derivative of x, y, A with respect to $(\ln a)$, we find the following autonomous system

$$\frac{dx}{d(\ln a)} = -2x(3 + y + xy), \quad (23)$$

$$\frac{dy}{d(\ln a)} = 2xy^2 \frac{V_{\phi\phi} V}{V_\phi^2} - y \frac{\ddot{\phi}}{\phi H} - y \frac{\dot{H}}{H^2}, \quad (24)$$

$$\frac{dA}{d(\ln a)} = -2xyA(1-A) \frac{V}{V_\phi \phi}, \quad (25)$$

which after the substitution of the relations (14), (15), (21), (22) has the final form

$$\frac{dx}{d(\ln a)} = -2x(3 + y + xy), \quad (26)$$

$$\begin{aligned} \frac{dy}{d(\ln a)} = 2xy^2 \left\{ 1 + \frac{(n-1)A^n}{mA^n - \frac{\lambda n}{M_{Pl}^n}(1-A)^n} - \frac{mnA^{2n}}{\left[mA^n - \frac{\lambda n}{M_{Pl}^n}(1-A)^n \right]^2} \right\} + y(9/2 + y + 3w/2) - \\ - \frac{xy^3}{M_{Pl}^2} A^{2n-2} (x(w-1) + w+1) \left[\frac{1-A}{mA^n - \frac{\lambda n}{M_{Pl}^n}(1-A)^n} \right]^2, \end{aligned} \quad (27)$$

$$\frac{dA}{d(\ln a)} = - \frac{2xyA^{n+1}(1-A)}{mA^n - \frac{\lambda n}{M_{Pl}^n}(1-A)^n}. \quad (28)$$

Once the autonomous system of equations is set up, we can proceed for its analysis that we do in the following subsections.

B. Stationary points

Solving the system (26)-(28), we find the stationary points and investigate their stability in the linear approximation *a la* Lyapunov [44]. In this case, there exist four fixed points.

1. $x = 0, y = 0, A \in (-\infty; +\infty)$.

This is stationary line. Eigenvalues of the Jacobian matrix associated with the system (26)-(28) are given by,

$$\begin{aligned} L_1 &= -6 < 0, \\ L_2 &= 9/2 + 3w/2 > 0 \quad \text{for } w \in [-1; 1], \\ L_3 &= 0 \end{aligned} \quad (29)$$

The eigenvalues L_2 is positive for $w \in [-1; 1]$, hence this stationary line is unstable. We calculate corresponding values of the important quantities (14), (15): $\frac{\dot{H}}{H^2} = -\frac{3}{2}(w+1)$, $\frac{\dot{\phi}}{\phi H} = -3$. Then $H(t) = \frac{2}{3(w+1)(t-t_0)}$, $\frac{d(\phi)}{\phi} = -3H(t)dt$ and

$$\dot{\phi}(t) = \phi_1(t-t_0)^{-\frac{2}{w+1}}, \quad (30)$$

$$\phi(t) = \phi_0 + \phi_1 \frac{w+1}{w-1} (t-t_0)^{\frac{w-1}{w+1}}, \quad (31)$$

the time dependence of the scale factor is

$$a(t) = a_0(t-t_0)^{\frac{2}{3(w+1)}}. \quad (32)$$

Using the continuity equation $\dot{\rho} + 3(w+1)H\rho = 0$ we find the time dependence of the energy density of matter

$$\rho(t) = \rho_0(t-t_0)^{-2}. \quad (33)$$

Here $t_0, \phi_0, \phi_1, \rho_0$ are constants.

The coordinate of this stationary line do not allow us to reconstruct correctly the behavior of the scalar field $\phi(t)$ and the formula (31) is very inexact. Our numerical investigations (see the next Section) confirm the power-law dependence $\dot{\phi}(t)$ in (30), however, the absolute value of $\dot{\phi}$ is very small, close to zero and $\phi(t)$ changes very slowly and equals approximately to the constant ϕ_0 .

Substituting values of coordinates of this stationary line to formulas (16), (17) we obtain $w_\phi \rightarrow -1$ and $w_{eff} \rightarrow w$. As the coordinate A run along an axis of real numbers then the parameter $\Gamma = \Gamma(A)$ (see (21)) can equal various values and we have $\Gamma = 1$ for the point of this line with $A = 0$.

In particular case of $w = -1$ instead the solution (31)-(33) we obtain from (14), (15) that Hubble parameter $H = H_0$, the matter energy density $\rho = \rho_0$, the time derivative of the scalar field decreases as the exponent $\dot{\phi}(t) = \phi_1 e^{-3H_0(t-t_0)}$ and the scalar field tends to constant $\phi(t) = \phi_0 - \frac{\phi_1}{3H_0} e^{-3H_0(t-t_0)} \rightarrow \phi_0$.

2. $x = 0, y = -9/2 - 3w/2, A \in (-\infty; +\infty)$.

We find eigenvalues for this stationary line

$$\begin{aligned} L_1 &= 3 + 3w \geq 0 & \text{for } w \in [-1; 1], \\ L_2 &= -9/2 - 3w/2 < 0 & \text{for } w \in [-1; 1], \\ L_3 &= 0 \end{aligned} \quad (34)$$

This stationary line is unstable for $w \in (-1; 1]$. We get the time behavior of the scale factor and $\dot{\phi}(t)$ calculating (14), (15): $\frac{\dot{H}}{H^2} = -\frac{3}{2}(w+1)$, $\frac{\dot{\phi}}{\phi H} = \frac{3}{2}(w+1)$. Then

$$\dot{\phi}(t) = \phi_1(t-t_0), \quad (35)$$

$$\phi(t) = \phi_0 + \phi_1(t-t_0)^2, \quad (36)$$

$$a(t) = a_0(t-t_0)^{\frac{2}{3(w+1)}}, \quad (37)$$

$$\rho(t) = \rho_0(t-t_0)^{-2}, \quad (38)$$

where $t_0, \phi_0, \phi_1, \rho_0$ are constants.

Using the numerical integration we confirm the time dependences of the scalar field derivative (35) and the difference $\phi(t) - \phi_0 = \phi_1(t-t_0)^2$. It is found that $|\dot{\phi}|$ close to zero and $\phi(t) \approx \phi_0$.

Applying formulas (16), (17) it is calculated that $w_\phi \rightarrow -1$ and $w_{eff} \rightarrow w$ in this line. The parameter Γ equals to 1 for the point of this stationary line with the coordinate $A = 0$.

For $w = -1$ the solution (36)-(38) does not exist and we find using (14), (15): $H = H_0, \rho = \rho_0, \dot{\phi}(t) = \phi_1$. The numerical integration gives us that $\dot{\phi}(t) = \phi_1 \approx 0$ and the scalar field equals to constant $\phi(t) \approx \phi_0$.

3. $x = \frac{1+w}{1-w}$, $y = -3/2 + 3w/2$, $A = 0$.

This point corresponds to the scaling solution and it exists for $w \neq 1$ (for realistic fluid, $w = 0; 1/3$). We are specially interested in this case, the eigenvalues are

$$\begin{aligned} L_1 &= 0, \\ L_{2,3} &= 3/4 \left(w - 1 \pm \sqrt{(9w+7)(w-1)} \right). \end{aligned} \quad (39)$$

Real parts of eigenvalues L_2, L_3 are negative for $w \in (-1; 1)$. As L_1 vanishes, one needs an additional check for the determination of the type of stability.

Since the coordinate $x = \frac{1+w}{1-w} = \frac{\phi^2}{2V} \geq 0$ for $w \in [-1; 1)$ then $V(\phi) > 0$ and the conditions of existence of the scaling point are

- 1). m is even, $\forall \phi$,
- 2). m is odd, $\phi > 0$.

Using formulas (14), (15), we find,

$$\frac{\dot{H}}{H^2} = -\frac{3}{2}(w+1) \quad (40)$$

$$\frac{\ddot{\phi}}{\dot{\phi}H} = -\frac{3}{2}(w+1). \quad (41)$$

Then

$$\dot{\phi}(t) = \phi_1(t-t_0)^{-1}, \quad (42)$$

$$a(t) = a_0(t-t_0)^{\frac{2}{3(w+1)}}, \quad (43)$$

$$\rho(t) = \rho_0(t-t_0)^{-2}, \quad (44)$$

where t_0, ϕ_1, ρ_0 are constants. Substituting values of coordinates of this stationary point to in (16), (17), (20), (21), we readily check that, $w_\phi \rightarrow w$, $w_{eff} \rightarrow w$, $\Omega_\phi \rightarrow 0$, $\Gamma \rightarrow 1$ as the fixed point is approached.

The numerical integration of the system (26)-(28) (see Figs. 1-3) are shown that the scaling stationary point **3** is the attractor in the phase space (x, y, A) for $(\ln a) \rightarrow +\infty$ in some region of the initial data. Therefore, the scaling regime (42)-(44) exists for $t \rightarrow +\infty$ and we can neglect t_0 .

The time behavior of the scalar field $\phi(t)$ cannot be found correctly from the coordinates of this stationary point.

Following [9], where the potential $V(\phi) = V_0 e^{-\frac{\lambda\phi^n}{M_{Pl}^n}}$ was considered, we assume for the potential (2) that the time dependence of $\phi(t)$ is given by the following series,

$$\lambda \left(\frac{\phi}{M_{Pl}} \right)^n = f_0 \ln \left(\frac{t}{t_1} \right) + f_1 \ln \ln \left(\frac{t}{t_1} \right) + \dots, \quad (45)$$

where f_0, f_1, t_1 are constants. Substituting this form of the scaling solution (43)-(45) to the equation (5) and using that $V_\phi = V_0 \phi^{m-1} e^{-\frac{\lambda\phi^n}{M_{Pl}^n}} \left(m - \frac{\lambda n}{M_{Pl}^n} \phi^n \right) \rightarrow V_0 \phi^{m-1} e^{-\frac{\lambda\phi^n}{M_{Pl}^n}} \left(-\frac{\lambda n}{M_{Pl}^n} \phi^n \right)$ for $\phi^n \rightarrow \infty, t \rightarrow +\infty$ we obtain

$$\frac{M_{Pl} f_0^{\frac{1}{n}} t_1 \left[\ln \left(\frac{t}{t_1} \right) \right]^{\frac{1}{n}-1}}{\lambda^{\frac{1}{n}} n t^2} \left(-1 + \frac{2}{w+1} \right) - V_0 n \left(\frac{M_{Pl}}{\lambda^{\frac{1}{n}}} \right)^{m-1} f_0^{\frac{m+n-1}{n}} t_1^{f_0} t^{-f_0} \left[\ln \left(\frac{t}{t_1} \right) \right]^{\frac{m+n-1}{n}-f_1} = 0. \quad (46)$$

Equalling the power-law indices and the coefficients of these two terms we find values of f_0, f_1, t_1 :

$$f_0 = 2, \quad f_1 = \frac{2n-2+m}{n}, \quad t_1 = \frac{M_{Pl}^{2-m}(1-w)}{V_0 n^2(1+w)} 2^{\frac{2-n-m}{n}} \lambda^{\frac{m-2}{n}}. \quad (47)$$

We note that for $w = -1$ coordinates x, y of this fixed point and the stationary line **2** coincide and we have the same behavior cosmological quantities: $H = H_0, \rho = \rho_0, \dot{\phi}(t) = \phi_1 \approx 0, \phi(t) \approx \phi_0$, where $\phi_1 \approx 0$ is found by the numerical investigations.

$$4. \quad x = -\frac{m(1+w)}{wm-m+4}, \quad y = \frac{3(wm-m+4)}{2(m-2)}, \quad A = 1.$$

This stationary point exists for $m \neq 0$, $m \neq 2$, $w \neq \frac{m-4}{m}$. Eigenvalues are found

$$\begin{aligned} L_1 &= -\frac{3(1+w)}{m-2} < 0 \quad \text{for } m > 2, w \in (-1; 1], \\ L_{2,3} &= \frac{3}{4(m-2)} \left(f_1(m, w) \pm \sqrt{f_2(m, w)} \right) \quad \text{Re}(L_{2,3}) < 0 \quad \text{for } m > 2, w \in \left(-1; \frac{m-6}{m+2}\right), \end{aligned} \quad (48)$$

where $f_1(m, w) = w(m+2) - m + 6$,

$$f_2(m, w) = (9m^2 - 12m + 4)w^2 + 2(20m - m^2 - 20)w - 7m^2 + 36m - 28.$$

We note that the function $f_1(m, w) < 0$ for $w < \frac{m-6}{m+2}$, while $f_2(m, w) < 0$ for $w_1 < w < w_2$

$$\text{where } w_{1,2} = \frac{20+m^2-20m \mp 8\sqrt{(m-1)(m-2)^3}}{(3m-2)^2}.$$

Thus the imaginary parts of the eigenvalues $L_{2,3}$ appear for $w_1 < w < w_2$.

We find that $w_1 < \frac{m-6}{m+2} < w_2$. Moreover, when $w \leq w_1$ the eigenvalues $L_3 < L_2 < 0$; when $w \geq w_2$ the eigenvalue $L_2 > 0$. Therefore, taking account that $L_1 < 0$ for $m > 2$, $w \in (-1; 1]$, we obtain the stability conditions of the point 4: it is a stable node for $w \in (-1; w_1]$, $m > 2$ and a stable focus for $w \in \left(w_1; \frac{m-6}{m+2}\right)$, $m > 2$.

For example, for a ordinary matter $w = 0$, stable point exists when $m > 6$ and for radiation, $w = \frac{1}{3}$ stable point exists when $m > 10$. For $2 < m < 6$, this point behaves like unstable (saddle) for both radiation and matter. For the case $m = 6$, with $w = 0$ it behaves like a centre and for $w = \frac{1}{3}$ it behaves like a saddle point.

The coordinate x of this fixed point can be both positive and negative depending on m , w . Taking into account the definition of $x = \frac{\dot{\phi}^2}{2V}$ we find the conditions of existence of this point:

- 1). m is even, $\forall \phi$ or m is odd, $\phi > 0$ and $w \in \left[-1; \frac{m-4}{m}\right)$,
- 2). m is odd, $\phi < 0$ and $w \in \left(\frac{m-4}{m}; 1\right]$.

Since $\frac{m-4}{m} > \frac{m-6}{m+2}$ for $m > 2$ then for odd m and $\phi < 0$ the point 4 is unstable.

Time behavior of the scale factor, scalar field and the energy density of matter are calculated in the same way as for the previous fixed points. Since $\frac{\dot{H}}{H^2} = -\frac{3}{2}(w+1)$, $\frac{\dot{\phi}}{\phi H} = \frac{3m(1+w)}{2(2-m)}$, we find $\dot{\phi}(t) = \phi_1(t-t_0)^{\frac{2m}{2-m}}$. Therefore, there is the following solution in this stationary point

$$\phi(t) = \phi_0(t-t_0)^{\frac{2}{2-m}}, \quad (49)$$

$$a(t) = a_0(t-t_0)^{\frac{2}{3(w+1)}}, \quad (50)$$

$$\rho(t) = \rho_0(t-t_0)^{-2}, \quad (51)$$

where t_0 , ϕ_0 , ϕ_1 , ρ_0 are constants. As the fixed point coordinate $A \rightarrow 1$ then the scalar field ϕ tends to zero in the found asymptotic solution (49)-(51). Therefore, it exists for $0 < m < 2$, $t \rightarrow t_0$ or $m > 2$, $t \rightarrow +\infty$. The constant ϕ_0 is found after the substitution this solution (49)-(51) to the Eq. (5)

$$\frac{2m}{(2-m)^2} \phi_0(t-t_0)^{\frac{2(m-1)}{2-m}} + \frac{4}{(2-m)(1+w)} \phi_0(t-t_0)^{\frac{2(m-1)}{2-m}} \phi_0 + V_0 m \phi_0^{m-1} (t-t_0)^{\frac{2(m-1)}{2-m}} = 0, \quad (52)$$

where we have used that $V_\phi = V_0 \phi^{m-1} e^{\frac{-\lambda \phi^n}{M_{Pl}^n}} \left(m - \frac{\lambda n}{M_{Pl}^n} \phi^n\right) \rightarrow V_0 m \phi^{m-1}$ for $\phi \rightarrow 0$. From (52) it follows

$$\phi_0^{m-2} = \frac{2(m(1-w)-4)}{V_0 m(1+w)(2-m)^2}. \quad (53)$$

Using values of coordinates of this stationary point it is obtained that $\Gamma \rightarrow \frac{m-1}{m}$, $w_\phi \rightarrow \frac{wm+2}{m-2}$, $w_{eff} \rightarrow w$. In the discussion to follow, we shall numerically confirm the aforesaid results based upon linear approach.

For $w = -1$ we have the same situation as in the previous point: $H = H_0$, $\rho = \rho_0$, $\dot{\phi}(t) = \phi_1 \approx 0$, $\phi(t) \approx \phi_0$, where $\phi_1 \approx 0$ is obtained numerically.

III. NUMERICAL INVESTIGATIONS

In the preceding section, we found the fixed points of the dynamical system under consideration and discussed their stability. In what follows we shall confirm the details using numerical integration of equations of motion. We integrate numerically two first-order systems of differential equations for several sets of fixed parameters $n > 1$, $m \geq 0$, $\lambda > 0$, $V_0 > 0$:

(1) The system with initial variables ϕ , $\Phi = \dot{\phi}$, H , which is derived from (3)-(5)

$$\frac{d\phi}{d(\ln a)} = \frac{\Phi}{H}, \quad (54)$$

$$\frac{d\Phi}{d(\ln a)} = -3\Phi - \frac{V_0 e^{-\frac{\lambda\phi^n}{M_{Pl}^n}}}{H} \left(m\phi^{m-1} - \frac{\lambda n}{M_{Pl}^n} \phi^{m+n-1} \right), \quad (55)$$

$$\frac{dH}{d(\ln a)} = -\frac{1}{2M_{Pl}^2 H} \left[\Phi^2 + (1+w) \left(3M_{Pl}^2 H^2 - \frac{\Phi^2}{2} - V_0 \phi^m e^{-\frac{\lambda\phi^n}{M_{Pl}^n}} \right) \right], \quad (56)$$

where $\frac{d}{d(\ln a)} \equiv \frac{d}{H dt}$ and $\rho = 3M_{Pl}^2 H^2 - \frac{\Phi^2}{2} - V_0 \phi^m e^{-\frac{\lambda\phi^n}{M_{Pl}^n}}$ have been substituted;

(2) The autonomous system with dimensionless variables x , y , A (26)-(28).

We compare the results obtained from both the systems, which are presented in Figs. 3-9. Let us mention that it is convenient to use the system with original variables also to compute the behavior of certain physical quantities like ρ_ϕ ; it also provides a cheque of results obtained using the autonomous form.

Trajectories in the phase space (x, y, A) are plotted using the system with variables x , y , A (26)-(28) and they are shown in Figs. 3-5 (left). Right pictures in Figs. 3-5 and Fig. 8 (left) demonstrate the evolution of variables x , y , A , which are obtained by applying the initial equations of motion (54)-(56). In Figs. 3-5 (right) we see that the variables x , y , A approach the coordinates specific to the scaling point for large values of $(\ln a)$ that is at late times. The scaling stationary point **3** has the complex type of stability (see left Fig. 5). This is stable for some initial data (black trajectories go to the point **3**) and unstable for others (green trajectories leave from the scaling point **3** and go to infinity).

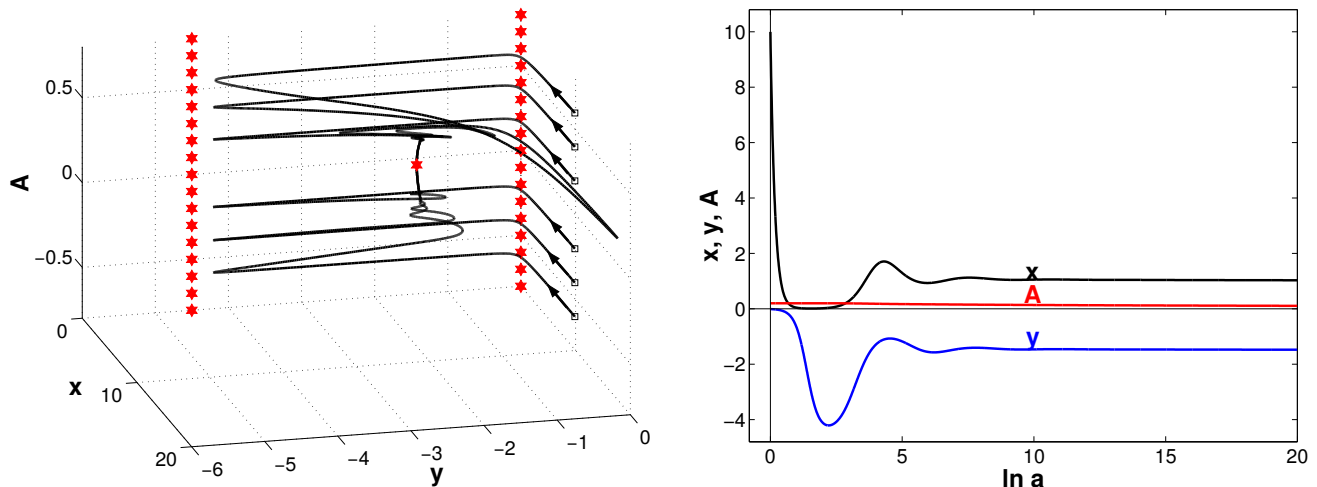


FIG. 3. Several trajectories in the phase space (x, y, A) (left) and the evolution of variables x , y , A (right). In the left plot vertical straight lines of red stars are stationary lines **1**, **2**. The separate red star is the scaling solution point **3**. Squares in the denote initial data, which are chosen $x(0) = 10$, $y(0) = -0.01$, $A(0)$ from -0.6 to -0.2 with step 0.2 and from 0.2 to 0.6 with step 0.2 . For the right graph starting values are $\phi(0) = 4$, $\dot{\phi}(0) = 0.0015$, $H(0) = 0.06$. Parameters are $n = 2$, $m = 0$, $V_0 = 1$, $\lambda = 1$, $w = 0$, $M_{Pl}^2 = 1$.

Secondly, for $m > 2$, $w \in \left(-1; \frac{m-6}{m+2}\right)$, there exists one more attractor, namely, the fixed point **4** in addition to point **3** (the scaling solution). This case is illustrated in left Figs. 4, 5. Before reaching of one of two attractors the

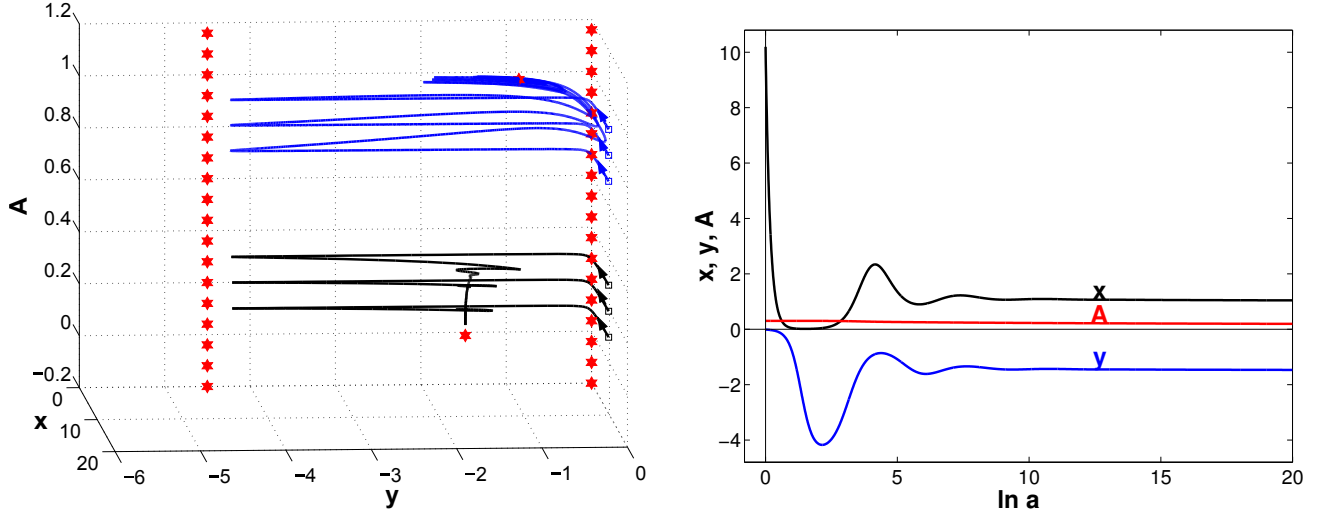


FIG. 4. Several trajectories in the phase space (x, y, A) (left) and the evolution of variables x, y, A (right). In the left graph vertical straight lines of red stars are stationary lines **1, 2**. The separate red stars are the scaling solution point **3** and the point **4**. Squares denote initial data, which are chosen $x(0) = 10$, $y(0) = -0.01$, $A(0)$ from 0.1 to 0.3 with step 0.1 for black curves and $x(0) = -10$, $y(0) = -0.01$, $A(0)$ from 0.7 to 0.9 with step 0.1 for blue curves. For the right plot starting values are $\phi(0) = 2.3$, $\dot{\phi}(0) = 0.19$, $H(0) = 10$. Parameters are $n = 3$, $m = 7$, $V_0 = 1$, $\lambda = 1$, $w = 0$, $M_{Pl}^2 = 1$.

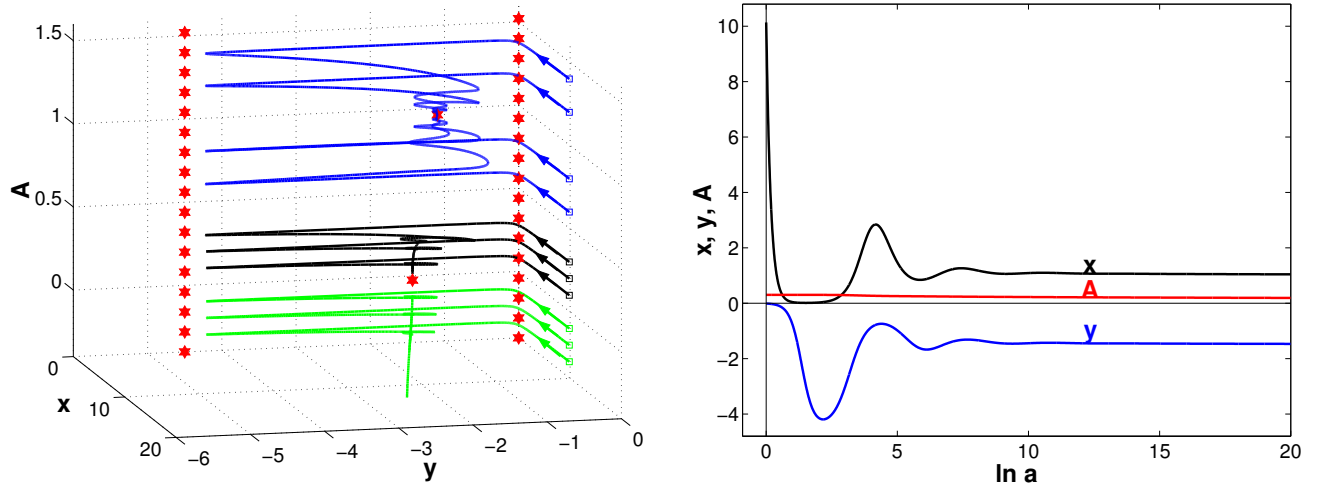


FIG. 5. Several trajectories in the phase space (x, y, A) (left) and the evolution of variables x, y, A (right). In the left graph vertical straight lines of red stars are stationary lines **1, 2**. The separate red stars are the scaling solution point **3** and the point **4**. Squares denote initial data, which are chosen $x(0) = 10$, $y(0) = -0.01$, $A(0)$ from 0.1 to 0.3 with step 0.1 for black curves, $x(0) = 10$, $y(0) = -0.01$, $A(0) = 0.6; 0.8; 1.2; 1.4$ for blue lines and $x(0) = -10$, $y(0) = -0.01$, $A(0)$ from -0.3 to -0.1 with step 0.1 for green curves. For the right plot starting values are $\phi(0) = 2.3$, $\dot{\phi}(0) = 1.52$, $H(0) = 70$. Parameters are $n = 3$, $m = 12$, $V_0 = 1$, $\lambda = 1$, $w = 0$, $M_{Pl}^2 = 1$.

trajectories move from the stationary line **1** to **2**, each point of which is a saddle. Then the trajectories of black colour go to the stable point **3** and blue those go to the point **4**. In Fig. 8 the evolution of x, y, A is shown, which corresponds to blue curves in Fig. 5. The variables x, y, A approach their values in the fixed point **4** at late times ($\ln a \rightarrow +\infty$).

Further, integrating the initial system, we plot the dependence of quantities $\phi, \rho, \rho_\phi, \Gamma, w_\phi, \Omega_\phi$ versus $(\ln a)$ in Figs. 6-9. When the phase trajectories move near the stationary lines **1** and **2** the scalar field ϕ behaves almost like a constant, changing very slowly. It is seen from the left plot in Fig. 6 and the middle graph in Fig. 8 at the initial stages of the evolution $\phi(\ln a)$. We reveal numerically the power-law dependences of scalar field derivative $\dot{\phi}$ the same

as in (30), (35) and the behavior of the scalar field ϕ near the stationary line **2**, which coincides with (36), and find that $|\dot{\phi}| \approx 0$ at both stationary lines.

At $\ln a \rightarrow +\infty$ the scalar field ϕ , the matter energy density ρ and other said quantities display behaviors corresponding to the asymptotic scaling solution (43)-(45) (see Figs. 6, 7) or to the power-law asymptotic regime (49)-(51) (see Figs. 8, 9) depending on initial conditions. We note that a power-law function in double logarithmic scale is a straight line. In the scaling solution the scalar field ϕ increases as $(\ln a)^\alpha$, the energy densities ρ and ρ_ϕ decrease as the scale factor a in different degrees, the parameter Γ tends to unity, the parameter of the scalar field equation of state w_ϕ approaches to w and Ω_ϕ decays as $(\ln a)^\beta$, where $\alpha = \frac{1}{n}$, $\beta = \frac{2-n}{n}$ are power indices calculated from (45). In the power-law solution ϕ , ρ , ρ_ϕ , Ω_ϕ decrease as the scale factor in some degrees, Γ and w_ϕ tend to constants $\frac{m-1}{m}$, $\frac{wm+2}{m-2}$ correspondingly. Therefore, we conclude that the result of the numerical investigation of the initial system coincide with calculations based upon (10)-(21), where coordinates of the fixed points **3** and **4** are substituted.

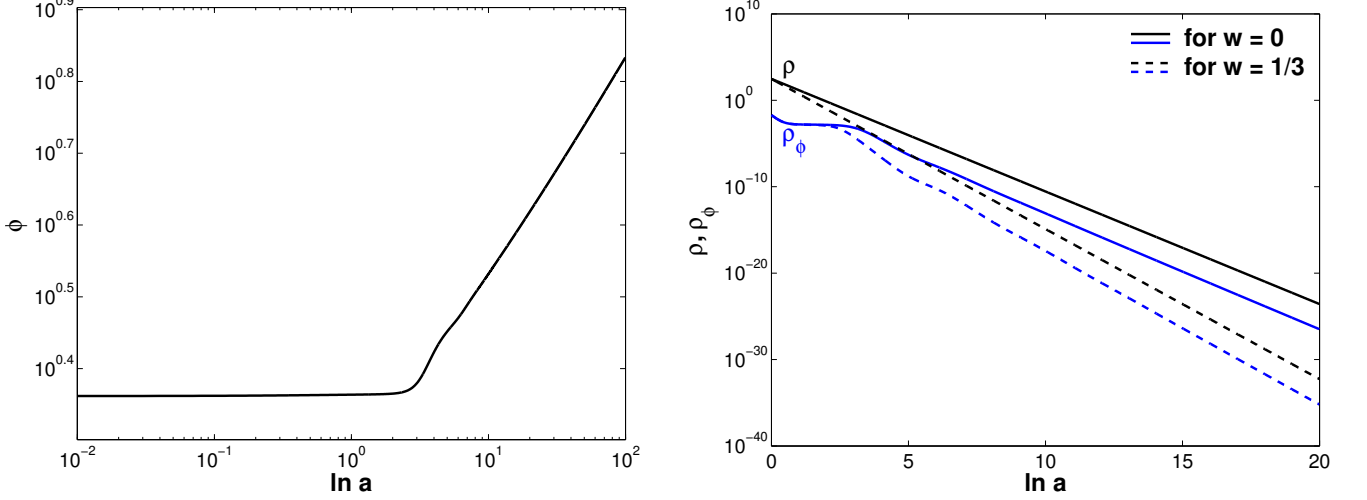


FIG. 6. There are the evolution of $\phi(\ln a)$ in the left plot, $\rho_\phi(\ln a)$ (blue) in the right graph for initial data: $\phi(0) = 2.3$, $\dot{\phi}(0) = 0.19$, $H(0) = 10$. Parameters are $n = 3$, $m = 7$, $V_0 = 1$, $\lambda = 1$, $M_{Pl}^2 = 1$ for all curves, $w = 0$ for solid lines and $w = 1/3$ for dashed those.

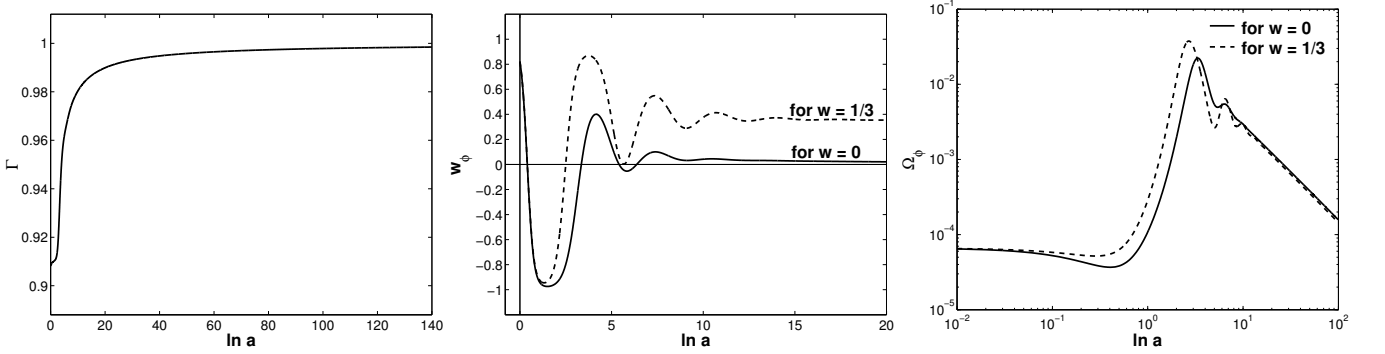


FIG. 7. There are the evolution of $\Gamma(\ln a)$ (left), $w_\phi(\ln a)$ (middle), $\Omega_\phi(\ln a)$ (right) for the same initial data and parameters as in Fig. 6.

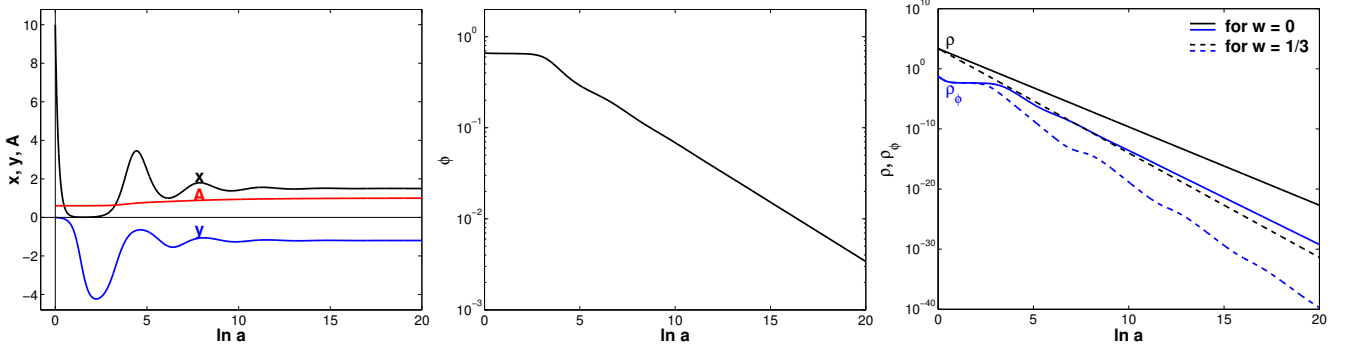


FIG. 8. There are the evolution of variables x, y, A in the left plot, $\phi(\ln a)$ in the middle graph, $\rho(\ln a)$ (black), $\rho_\phi(\ln a)$ (blue) in the right picture for initial data: $\phi(0) = 0.66$, $\dot{\phi}(0) = -0.32$, $H(0) = 28$. Parameters are $n = 3$, $m = 12$, $V_0 = 1$, $\lambda = 1$, $M_{Pl}^2 = 1$, $w = 0$.

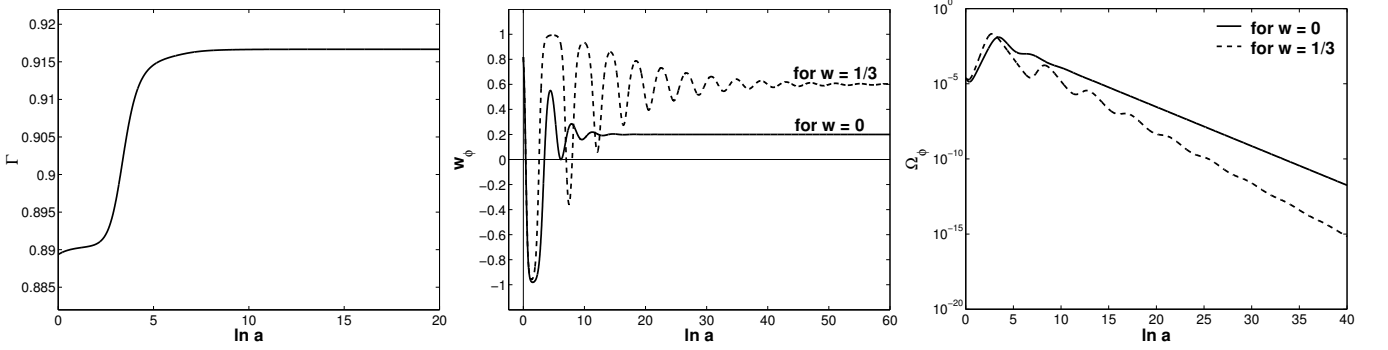


FIG. 9. Figure displays evolution of $\Gamma(\ln a)$ (left), $w_\phi(\ln a)$ (middle), $\Omega_\phi(\ln a)$ (right) for the same initial data and parameters as in Fig. 8.

IV. CONCLUSION

In this paper we have investigated cosmological dynamics of scalar field ϕ with $V(\phi) = V_0 \phi^m \text{Exp}(-\lambda \phi^n / M_{Pl}^n)$; $m \geq 0$, $n > 1$ in the presence of background matter. We used the autonomous system with three variables x, y and A which govern the dynamics of the underlying system. In addition, we also used the dynamical system (3)-(5) with original variables; the latter was convenient to compute certain physical quantities like ρ_ϕ and also provided an independent cross check on results obtained using the autonomous system.

In case, $m = 0$ and $n = 1$, for which $\Gamma = V_{\phi\phi} V / V_\phi^2 = 1$, we have standard scaling solution which tracks the background matter as an attractor. In a general class potentials with $m \geq 0, n > 1$, we should mimic the said behavior in the asymptotic regime as $\Gamma = V_{\phi\phi} V / V_\phi^2 \rightarrow 1$ for $|\phi| \rightarrow \infty$. Indeed, in this case, we find three fixed points, namely, two fixed points given by $x = 0, y = 0, A = 0$ & $x = 0, y = -9/2 - 3w/2, A = 0$ which belong to two stationary lines; both of them are unstable solutions. As expected, we also have scaling solution with $A = 0$ corresponding to the third stationary point, which is stable for some limited region of the phase space, see the black trajectories in Fig. 3-5 (left). The type of stability of the scaling point is complicated. It is demonstrated in Fig. 5 (left), where the green curves go at first to the scaling point, then they leave it and go to infinite values of A . The scaling solution is reached asymptotically for $|\phi| \rightarrow \infty$ such that $w_\phi \rightarrow w$ ($V(\phi) \rightarrow 0, \Omega_\phi \rightarrow 0$). The left plot in Fig. 6 displays the behavior of ρ_ϕ in the presence of background matter. As seen in the figure, field being initially sub-dominant remains frozen till its energy density becomes comparable to the background energy density. Thereafter, the evolution of ρ_ϕ commences, ultimately catches up with the background, and tracks it forever *a la* the scaling regime.

The fourth fixed point is also stable for $w \in \left(-1; \frac{m-6}{m+2}\right)$, $m > 2$ and corresponds to $A = 1$ or $\phi = 0$ (see left plots in Figs. 4, 5, which show both fixed points **3** and **4** for which $\Omega_\phi \rightarrow 0$ and $w_{eff} \rightarrow w$. In this case, $w_\phi \rightarrow (wm+2)/(m-2)$ as the fixed point is reached; for $m = 12, w = 0, w_\phi \rightarrow 0.2$ and for $m = 12, w = 1/3, w_\phi \rightarrow 0.6$ (see Fig. 8 & 9). It is found that the stability of stationary point **4** does not depend on the existence of minimum of the potential at $\phi = 0$. For example, when $n = 3, m = 7$ the scalar field potential has not the minimum at $\phi = 0$ as it is shown in Fig. 2 (left) and, however, the stable fixed point **4** exists for $w < \frac{1}{9}$ (see the left graph in Fig. 5). Actually, the minimum of the

potential at $\phi = 0$ corresponds to the stable scalar field oscillations near zero. In the oscillation regime the variables x, y can go through the infinite values and, therefore, it cannot be revealed from the analysis of the dynamical system with those variables. Let us emphasize that the definition of autonomous variables are different from the standard ones not suitable to the investigation of the stability of de Sitter solution, we have added an Appendix B which separately deals with de Sitter case.³ It should be noted that the asymptotic behavior of Γ in the limit $|\phi| \rightarrow \infty$ for generalized exponential potential and the potential given by the expression (2) is the same, the contribution from the power law in the asymptotic regime is negligible. However, the fixed point 4 does not exist in case of generalized exponential potential. On the other hand, as well known, the scaling solution does not exist for $n = 0$ (the case of power-law potential) which is clarified in Appendix A for the framework used by us.⁴

During our investigation we had found that the standard choice of autonomous variables was cumbersome when applied to the potential (2). As demonstrated in Ref. [9], the model with $m = 0$ can reconcile easily with observational constraints on inflationary era as well as the late time acceleration making the latter independent of initial conditions *a la* the tracking behavior. In the generalized case, the desirable behavior is shown to be intact. We have rigorously shown the existence and stability of scaling solution using the fixed point analysis. Interestingly, we have demonstrated, as expected, that $\Omega_\phi \rightarrow 0$ as the scaling regime is reached asymptotically, thereby, the nucleosynthesis is taken care off naturally. Indeed, Figs. 6 & 7 clearly show, that ρ_ϕ tracks the background ultimately, showing the commencement of scaling regime such that $\Gamma \rightarrow 1$, $w_\phi \rightarrow w$ and Ω_ϕ diminishes compared to the background matter content. The said behavior is suited to unified models of inflation and late time acceleration. It should, however, be mentioned that the class of models under consideration on their own cannot account for late time acceleration. To that effect, we imagine the presence of an additional mechanism responsible for late time exit from scaling regime to accelerated expansion. As pointed out in Ref. [9], the interaction with massive neutrino matter may easily trigger the said transition at late stages. Finally, we should note that the model based upon the generalized class of potentials has richer structure than the one considered in Ref. [9] and deserves further attention for model building for quintessential inflation.

V. ACKNOWLEDGEMENT

We thank T. Padmanabhan for a remark on scaling behavior in the asymptotic regime. MS and NJ are supported by the Indo-Russia Project (INT/RUS/RFBR/P-315).

³ As demonstrated in Ref. [5], coupling of the field to massive neutrino matter triggers a minimum in the field potential giving rise to de Sitter solution which is a late time attractor of the dynamics.

⁴ It should be noted that the singular inflation scenarios exist [45] for scalar field models with the power-law potential.

VI. APPENDIX A: THE CASE OF $V(\phi) = V_0\phi^m$ ($n = 0$)

For $n = 0$ the scalar field potential is $V(\phi) = V_0\phi^m$ and the system (26)-(28) has the form

$$\frac{dx}{d(\ln a)} = -2x(3 + y + xy), \quad (57)$$

$$\frac{dy}{d(\ln a)} = 2xy^2 \frac{m-1}{m} + y(9/2 + y + 3w/2) - \frac{xy^3}{M_{Pl}^2 m^2} (x(w-1) + w+1) \left(\frac{1-A}{A} \right)^2, \quad (58)$$

$$\frac{dA}{d(\ln a)} = -\frac{2}{m} xyA(1-A). \quad (59)$$

We solve this system and find following stationary points.

1. $x = 0, y = 0, A \in (-\infty; +\infty)$.

This is stationary line. Eigenvalues are calculated

$$\begin{aligned} L_1 &= -6 < 0 \\ L_2 &= 9/2 + 3w/2 > 0 \quad \text{for } w \in [-1; 1] \\ L_3 &= 0 \end{aligned} \quad (60)$$

2. $x = 0, y = -9/2 - 3w/2, A \in (-\infty; +\infty)$.

We find eigenvalues for this stationary line

$$\begin{aligned} L_1 &= 3 + 3w \geq 0 \quad \text{for } w \in [-1; 1] \\ L_2 &= -9/2 - 3w/2 < 0 \quad \text{for } w \in [-1; 1] \\ L_3 &= 0 \end{aligned} \quad (61)$$

3. $x = -\frac{m(1+w)}{wm-m+4}, y = \frac{3(wm-m+4)}{2(m-2)}, A = 1$.

This stationary point exists for $m \neq 0, m \neq 2, w \neq \frac{m-4}{m}$. Eigenvalues are found

$$\begin{aligned} L_1 &= -\frac{3(1+w)}{m-2} < 0 \quad \text{for } m > 2, w \in (-1; 1], \\ L_{2,3} &= \frac{3}{4(m-2)} \left(f_1(m, w) \pm \sqrt{f_2(m, w)} \right) \quad \text{Re}(L_{2,3}) < 0 \quad \text{for } m > 2, w \in \left(-1; \frac{m-6}{m+2} \right), \end{aligned} \quad (62)$$

where $f_1(m, w) = w(m+2) - m + 6$,

$$f_2(m, w) = (9m^2 - 12m + 4)w^2 + 2(20m - m^2 - 20)w - 7m^2 + 36m - 28.$$

We see that the coordinates x and y of these stationary points are not equal to $\frac{1+w}{1-w}$ and $\frac{3}{2}(w-1)$, correspondingly. Therefore, the scaling solution does not exist in the model with the potential $V(\phi) = V_0\phi^m$.

VII. APPENDIX B: THE STABILITY OF DE SITTER SOLUTION

De Sitter solution $H = H_0, \phi = \phi_0, \rho = 0$ exists for

$$\begin{aligned} V_\phi(\phi_0) = V_0\phi_0^{m-1} e^{-\frac{\lambda\phi_0^n}{M_{Pl}^n}} \left(m - \frac{\lambda n}{M_{Pl}^n} \phi_0^n \right) = 0 &\Rightarrow \mathbf{1).} \phi_0 = 0, \mathbf{2).} \phi_0^n = \frac{mM_{Pl}^n}{\lambda n}, \\ 3H_0^2 M_{Pl}^2 = V_0\phi_0^m e^{-\frac{\lambda\phi_0^n}{M_{Pl}^n}} &\Rightarrow \mathbf{1).} H_0 = 0, \mathbf{2).} H_0^2 = \frac{V_0}{3M_{Pl}^2} \left(\frac{mM_{Pl}^n}{\lambda n} \right)^{\frac{m}{n}} e^{-\frac{m}{n}}. \end{aligned} \quad (63)$$

Adding small perturbations to this solution $\phi(t) = \phi_0 + \delta\phi, \dot{\phi}(t) = \delta\dot{\phi}, H(t) = H_0 + \delta H$ we substitute these to Eqs. (4), (5) and find in the linear approach

$$\delta\dot{H} = -3H_0(1+w)\delta H + \frac{V_\phi(\phi_0)(1+w)}{2M_{Pl}^2} \delta\phi, \quad (64)$$

$$\delta\ddot{\phi} + 3H_0\delta\dot{\phi} + V_{\phi\phi}(\phi_0)\delta\phi = 0, \quad (65)$$

where $\rho = 3H^2 M_{Pl}^2 - \frac{1}{2}\dot{\phi}^2 - V(\phi)$ has been substituted. We introduce new variables $s_1 = \delta\phi$, $s_2 = \delta\dot{\phi}$, $s_3 = \delta H$ and obtain first-order system of differential equations

$$\dot{s}_1 = s_2, \quad (66)$$

$$\dot{s}_2 = -3H_0 s_2 - V_{\phi\phi}(\phi_0) s_1, \quad (67)$$

$$\dot{s}_3 = -2H_0(1+w)s_3 + \frac{V_\phi(\phi_0)(1+w)}{2M_{Pl}^2} s_1. \quad (68)$$

The eigenvalues for the matrix of this system are

$$\begin{aligned} L_1 &= -3H_0(1+w) < 0 \quad \text{for } H_0 > 0, w \in (-1; 1], \\ L_{2,3} &= \frac{3}{2} \left(-H_0 \pm \sqrt{H_0^2 - 4V_{\phi\phi}(\phi_0)/9} \right) \quad \text{Re}(L_{2,3}) < 0 \quad \text{for } H_0 > 0, V_{\phi\phi}(\phi_0) > 0. \end{aligned} \quad (69)$$

Therefore, we have stable de Sitter solution in the minimum of the potential at $\phi = \phi_0$ (that is for $V_{\phi\phi}(\phi_0) > 0$).

-
- [1] P. G. Ferreira and M. Joyce, Phys. Rev. Lett. **79**, no. 24, 4740 (1997) [astro-ph/9707286].
[2] M. Sami and N. Dadhich, TSPU Bulletin **no. 7 (44)**, 25 (2004) [hep-th/0405016].
[3] V. Sahni, M. Sami and T. Souradeep, Phys. Rev. D **65**, no. 2, 023518 (2002) [gr-qc/0105121].
[4] H. Tashiro, T. Chiba and M. Sasaki, Class. Quant. Grav. **21**, no. 7, 1761 (2004) [gr-qc/0307068].
[5] M. W. Hossain, R. Myrzakulov, M. Sami and E. N. Saridakis, Int. J. Mod. Phys. D **24**, no. 05, 1530014 (2015) [arXiv:1410.6100 [gr-qc]].
[6] C. Q. Geng, M. W. Hossain, R. Myrzakulov, M. Sami and E. N. Saridakis, Phys. Rev. D **92**, no. 2, 023522 (2015) [arXiv:1502.03597 [gr-qc]].
[7] E. V. Linder, Rept. Prog. Phys. **71**, 056901 (2008) [arXiv:0801.2968 [astro-ph]].
[8] M. Sami, Curr. Sci. **97**, 887 (2009) [arXiv:0904.3445 [hep-th]].
[9] C.-Q. Geng, C.-C. Lee, M. Sami, E. N. Saridakis and A. A. Starobinsky, JCAP **06**, 011 (2017) [arXiv:1705.01329 [gr-qc]].
[10] P. J. E. Peebles and A. Vilenkin, Phys. Rev. D **59**, no. 6, 063505 (1999) [astro-ph/9810509].
[11] B. Spokoiny, Phys. Lett. B **315**, 40 (1993) [gr-qc/9306008].
[12] P. J. E. Peebles and A. Vilenkin, Phys. Rev. D **60**, no. 10, 103506 (1999) [astro-ph/9904396].
[13] M. Peloso and F. Rosati, JHEP **12**, 026 (1999) [hep-ph/9908271].
[14] K. Dimopoulos, Nucl. Phys. Proc. Suppl. **95**, 70 (2001) [astro-ph/0012298].
[15] E. J. Copeland, A. R. Liddle and J. E. Lidsey, Phys. Rev. D **64**, no. 2, 023509 (2001) [astro-ph/0006421].
[16] A. S. Majumdar, Phys. Rev. D **64**, no. 8, 083503 (2001) [astro-ph/0105518].
[17] M. Sami and V. Sahni, Phys. Rev. D **70**, no. 8, 083513 (2004) [hep-th/0402086].
[18] R. Rosenfeld and J. A. Frieman, JCAP **09**, 003 (2005) [astro-ph/0504191].
[19] K. Dimopoulos and J. W. F. Valle, Astropart. Phys. **18**, 287 (2002) [astro-ph/0111417].
[20] M. Giovannini, Phys. Rev. D **67**, no. 12, 123512 (2003) [hep-ph/0301264].
[21] S. Tsujikawa, Class. Quant. Grav. **30**, no. 21, 214003 (2013) [arXiv:1304.1961 [gr-qc]].
[22] M. W. Hossain, R. Myrzakulov, M. Sami and E. N. Saridakis, Phys. Rev. D **90**, no. 2, 023512 (2014) [arXiv:1402.6661 [gr-qc]].
[23] K. Dimopoulos and C. Owen, JCAP **06**, 027 (2017) [arXiv:1703.00305 [gr-qc]].
[24] Y. Akrami, R. Kallosh, A. Linde and V. Vardanyan, JCAP **06**, 041 (2018) [arXiv:1712.09693 [hep-th]].
[25] S. Ahmad, R. Myrzakulov and M. Sami, Phys. Rev. D **96**, no. 6, 063515 (2017) [arXiv:1705.02133 [gr-qc]].
[26] N. Jaman and K. Myrzakulov, arXiv:1807.07443 [gr-qc].
[27] M. W. Hossain, EPJ Web Conf. **168**, 04007 (2018) [arXiv:1801.03272 [gr-qc]].
[28] P. J. Steinhardt, L. Wang and I. Zlatev, Phys. Rev. D **59**, no. 12, 123504 (1999) [astro-ph/9812313].
[29] P. G. Ferreira and M. Joyce, Phys. Rev. D **58**, no. 2, 023503 (1998) [astro-ph/9711102].
[30] B. Ratra and P. J. E. Peebles, Phys. Rev. D **37**, no. 12, 3406 (1988).
[31] Z.-K. Guo, Y.-S. Piao and Y.-Z. Zhang, Phys. Lett. B **568**, 1 (2003) [hep-th/0304048].
[32] E. J. Copeland, M. Sami and S. Tsujikawa, Int. J. Mod. Phys. D **15**, no. 11, 1753 (2006) [hep-th/0603057].
[33] P. Singh, M. Sami, N. Dadhich, Phys. Rev. D **68**, no. 2, 023522 (2003) [hep-th/0305110].
[34] C. Wetterich, Phys. Rev. D **89**, no. 2, 024005 (2014) [arXiv:1308.1019 [astro-ph.CO]].
[35] R. R. Caldwell, R. Dave and P. J. Steinhardt, Phys. Rev. Lett. **80**, no. 8, 1582 (1998) [astro-ph/9708069].

- [36] M. Sami, *Models of Dark Energy*, In: Papantonopoulos L. (eds) *The Invisible Universe: Dark Matter and Dark Energy*. Lecture Notes in Physics, Vol. 720, pp. 219-256 (Springer, Berlin, Heidelberg, 2007).
https://www.ctp-jamia.res.in/people/models_of_dark_energy.pdf.
- [37] T. Chiba, Phys. Rev. D **81**, no. 2, 023515 (2010) [arXiv:0909.4365 [astro-ph.CO]].
- [38] M. Sami, arXiv:0901.0756 [hep-th].
- [39] F. Lucchin and S. Matarrese, Phys. Rev. D **32**, no. 6, 1316 (1985).
- [40] M. Sami, P. Chingangbam and T. Qureshi, Phys. Rev. D **66**, no. 4, 043530 (2002) [hep-th/0205179].
- [41] B. Ratra, Phys. Rev. D **45**, no. 6, 1913 (1992).
- [42] P. Parsons and J. D. Barrow, Phys. Rev. D **51**, no. 12, 6757 (1995) [astro-ph/9501086].
- [43] J. Rubio and C. Wetterich, Phys. Rev. D **96**, no. 6, 063509 (2017) [arXiv:1705.00552 [gr-qc]].
- [44] S. Wiggins, *Introduction to Applied Nonlinear Dynamical Systems and Chaos*. (Springer, New York, 1990).
- [45] J. D. Barrow and A. A. H. Graham, Phys. Rev. D **81**, no. 8, 083513 (2015) [arXiv:1501.04090 [gr-qc]].